International Journal of Fracture Fatigue and Wear, Volume 4

Proceedings of the 5th International Conference on
Fracture Fatigue and Wear, pp. 50-57, 2016

ELASTOPLASTIC FRETTING WEAR BEHAVIOUR OF CONTACT WIRES

T. Yue[1], D. Wang[2] and M. Abdel Wahab[1]

[1]Soete Laboratory, Faculty of Engineering and Architecture, Ghent University, Belgium
[2]School of Mechatronic Engineering, China University of Mining and Technology, Xuzhou 221116 China

Abstract: Fretting wear is damage caused by small movement between contact surfaces and imposed normal load. It occurs more seriously in gross sliding condition. Wire ropes in mine hoisting are typical examples where fretting wear occurs. This fretting damage causes stress concentration and accelerates the failure of ropes by decreasing cross section area. Considering the difficulties in monitoring stresses in experiments, finite element method (FEM) is a suitable numerical method to study the detail of this process. However, there is scarce information on the effect of material property on fretting wear of wire ropes in FEM. In this study, based on the FE model of wires, the FE results are validated with analytical solution and experiments. Then, the fretting loops and wear depth after 1000 cycles from different material behaviours are analysed. The results show that under elastic material behaviour, FEM has a good agreement with Hertzian solution. In addition, the wear depth obtained by FEM is close to experimental one. However, the fretting loop is a typical gross sliding shape in contrast to the experimental findings. For elastic perfectly plastic condition, the shape of fretting loop after 1000 cycles is same as that for elastic one, but the dissipated energy is higher. Moreover, the wear depth and wear scar calculated by plasticity is different from the elastic condition.

Keywords: Fretting wear, FEM, Material behaviour

1 INTRODUCTION

Fretting is small movement between contact surfaces. Depending on different loading conditions, namely combinations of normal load and oscillation, it could result in fretting fatigue in partial slip condition or fretting wear in gross sliding condition. The wire rope in mine hoisting is a typical example, in which fretting damage occurs due to the micro displacement of individual wires against their adjacent wires when the ropes are under axial cyclic stretching load and cyclic bending load. This causes stress concentration and accelerates the failure of ropes by decreasing of cross section area [1-3]. Previously, Wang et al. studied the influence of kinematic parameters of mine hoist on fretting parameters of the hoisting rope model [4], effects of displacement on fretting damage of wires in low cycle fatigue condition [5] and the influence of pH value in the corrosive media on fretting wear and fatigue life of wires [6]. This global hoisting rope model shows hoisting is a complex process, and experiments present complicated interaction of fretting wear and fretting fatigue. However, due to its micro displacement and micro size of debris, it is difficult to investigate the evolution of contact surfaces in the process of fretting wear by experiments. Therefore, researchers turn to numerical modelling, e.g. finite element method (FEM), to study the detail of this process. Cruzado et al. [7] firstly simulated the process of fretting wear in wires in a 90° crossed elastic cylinders configuration, then studied the influence of fretting wear on fatigue life of wires [8]. In their recent research[9], crossed-cylinder models of different angles under fretting condition were simulated, of which results showed good agreement with experimental data. Besides fretting model of wires, Wang [10] firstly studied stress distribution and fretting fatigue parameters of two upscale structures, i.e. 6×19 + IWS rope and $(1 + 6 + 12)$ strand with three layered strands to investigate the global response of rope in axially load condition and the influence of fretting wear on fretting scar. However, the process of fretting wear was calculated by the analytical solution instead of instantaneous contact pressure and relative slip of each increment, which are of importance in fretting wear simulations.

Though FEM could give a good agreement with experiments, the effect of material property on fretting wear has not been considered. However, assuming that the material is elastically deformed, which is usually defined in fretting wear simulations, underestimates the displacement for gross sliding in theoretical values [11]. Also, of a high friction coefficient fretting couple with typical tangential displacement, this high coefficient of friction is sufficient to cause plastic deformation in the contact surface [12].

In this paper, we investigated the influence of material property on fretting wear of wire ropes. The remainder of this paper is organized as follows. In section 2, the FE model used for the fretted wire is described, including geometry information and wears coefficient calculation. After that, the FE results are validated with analytical

solution and experiments. The fretting loops in elastic and elastic perfectly plastic conditions are analysed. Finally, the conclusion is summarized.

2 FE MODEL

2.1 Geometry information

According to the experimental set up in [13], the diameter of wires in FE model is 1 mm and is made of cold drawn, high-quality carbon structure steel. The coefficient of friction μ between contact surfaces is kept constant as 0.12, when the normal load applied P is 9 N and the displacement amplitude is 5 μm. The material property is shown in Table 1. In this study, elastic condition and elastic-perfectly-plastic condition are used to compare results with experimental data.

Table 1 Material property of wire used in FE model[13]

Material	Young's modulus E (GPa)	Poisson ratio υ	Yield strength (GPa)
Steel wire	203	0.3	0.64

The configuration of two cylindrical wires with same material and radius crossed at 90° is generated in the commercial FE software ABAQUS/STANDARD, as shown in Fig. 1. Contact interaction between two wires is defined by surface to surface with finite sliding contact pair algorithm, in which master–slave algorithm is used to search for the contact pair. Herein, the surface of upper wire is master surface and the surface of the other wire is slave surface. Lagrange multiplier algorithm is chosen to solve the contact problem in order to obtain more accurate relative slip than in case of penalty method.

The normal load and boundary conditions with vertical movement are applied on the top wire by kinematic coupling to define rigid motion in a reference point during the whole simulation [14]. While for the bottom wire, the reciprocating displacement in x direction is imposed after applying normal load. The loading history here is the same as in [15] and is shown in Fig. 2. Element type C3D8 is chosen in the elastic model while C3D8R is used in the elastic perfectly plastic model. The mesh size in contact zone is $10 \times 10 \times 10$ μm in elastic model and $5 \times 10 \times 10$ μm in plastic model based on convergence study, respectively. The total number of cycles is 13000, and the jump cycle is chosen to be 1000 for balancing accuracy and efficiency. Energy model for fretting wear is used, and the procedure of that can be found in [15].

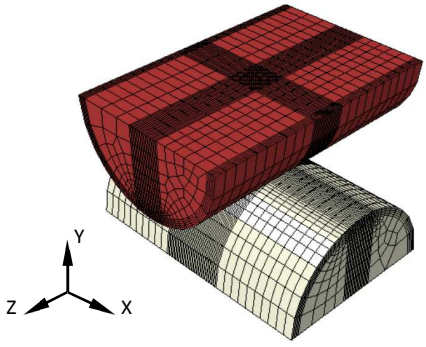

Fig. 1 The FE model of wire ropes

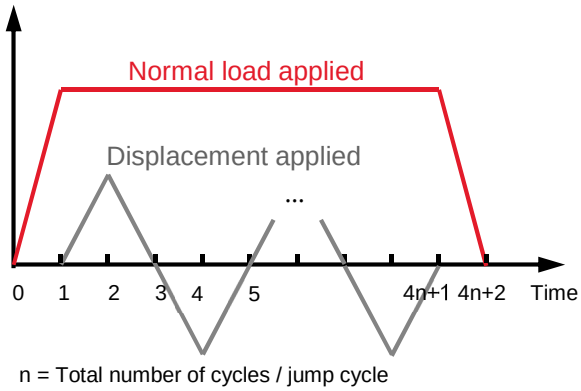

Fig. 2 Loading history adopted in FE model [15]

2.2 Wear coefficient calculation

Owning to lacking the Archard wear coefficient k in [13], wear coefficient calculated as follows [10, 16]:

For the two equal elastic cylinders with Young's modulus E and radius R crossed at right angle, the function of wear scar radius a with number of cycles N, applied normal load F and stroke Δx, is:

$$a = \sqrt[4]{a_0^4 + \frac{8kRP\Delta xN}{\pi}} \tag{1}$$

where a_0 is the Hertzian contact radius,

$$a_0 = 0.909\sqrt[3]{\frac{PR}{E}} \tag{2}$$

And the relation between fretting wear depth h_1 and a is given by:

$$h_1 = \frac{a^2 - a_0^2}{2R} \tag{3}$$

Therefore the Archard wear coefficient k could be obtained as:

$$k = \frac{[(2Rh_1 + a_0^2)^2 - a_0^4]\pi}{8RF\Delta xN} \tag{4}$$

Thus, energy wear coefficient k_E, based on Coulomb's friction law is obtained as:

$$k_E = \frac{[(2Rh_1 + a_0^2)^2 - a_0^4]\pi}{8RF\Delta xN\mu} \tag{5}$$

Therefore, k_E could be calculated based on h_1 measured. When $F = 9\ \mathrm{N}, \Delta x = 10\ \mu\mathrm{m}$, $h_1 = 1.89\ \mu\mathrm{m}$ from [13]. It should be mentioned that plastic deformation occurs in this loading condition based on FE result and material property. Fig. 3 shows that the maximum indentation displacement is $0.7\ \mu m$ due to plastic deformation. However, by experiments, it is difficult to separate plastic deformation from wear depth measurement. Therefore, in experiments, h_1 measured is the wear depth plus plastic deformation, where the depth due to plastic deformation is 37.6% of h_1 in this loading condition. Thus k_E calculated by h_1 is larger than the real situation. Considering this point, four conditions are simulated listed in Table 2. $k_E = 4.04 \times 10^{-8}\ MPa^{-1}$, is calculated by h_1, while $k_E = 2.09 \times 10^{-8}\ MPa^{-1}$ is obtained by the subtraction of the plastic displacement from h_1. Due to the convergence problem in plastic deformation of the whole period of fretting wear, the first 1000 cycles is studied here.

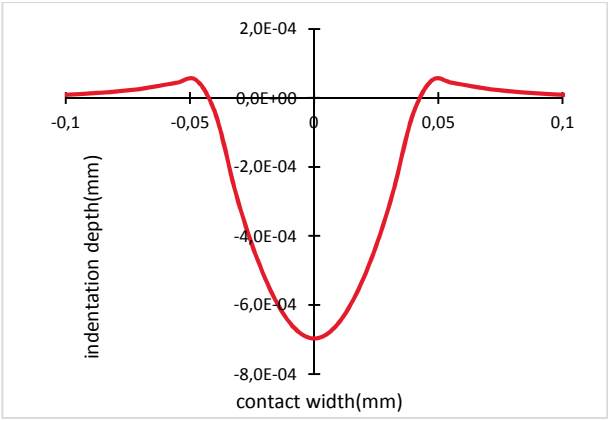

Fig. 3 The indentation depth of specimen surface in vertical direction from FEM, $\boldsymbol{F = 9\ \mathrm{N}, R = 0.5\ \mathrm{mm}}$

Table 2 key parameters on elastoplastic behaviour studying

No. of simulation	Number of cycles	k_E	Material behaviour
1	13000	4.04×10^{-8}	elastic
2	13000	2.09×10^{-8}	elastic
3	1000	4.04×10^{-8}	Elastic-perfectly-plastic
4	1000	2.09×10^{-8}	Elastic-perfectly-plastic

3 NUMERICAL RESULTS

3.1 Validation with Hertzian contact

Firstly, the elastic FE model is validated with Hertzian contact solution. Analytical formula in Hertzian contact for two equal cylinders with right angle is [17]:

Maximum contact pressure:

$$P_{max} = \sqrt[3]{\frac{6FE^2}{\pi^3 R^2}} \tag{6}$$

The comparison of FEA results and Hertzian solution is shown in Table 3. Both differences of P_{max} and contact radius are less than 5 %, which are in good agreement with each other.

Table 3 Comparison of FEA results and analytical solutions in $\boldsymbol{P_{max}}$ and $\boldsymbol{a_0}$

	Hertzian solution	FEA	Difference* (%)
P_{max} (MPa)	4454.54	4395	1.34
a_0 (mm)	0.0031	0.0029	4.8

*: Difference= (ABAQUS results – Hertzian solution) / Hertzian solution

3.2 Validation with experimental results

The first comparison of FEM and experimental results is wear depth after 13000 cycles. Table 4 lists the range of wear depth from experiments. According to [18], about 66.67% of the data points should be in the range of mean ± 1 standard deviation (SD), namely 1.5~2.3 μm, and about 95% of the data points will be within 2 SD of the mean that is 1.1~2.7 μm. The wear depth of bottom surface of simulation 1 and simulation 2 are depicted in Fig. 4. It is found that: in both cases, the distributions of wear depth along x and z directions are the same as each other. When $k_E = 4.04 \times 10^{-8}\ MPa^{-1}$, the wear depth is 2.7 μm and it is 1.77 μm with $k_E = 2.09 \times 10^{-8}\ MPa^{-1}$. Although both of the wear depths simulated are in the range of 2 SD, the $k_E = 2.09 \times 10^{-8}\ MPa^{-1}$ case is more reliable comparing the case of $k_E = 4.04 \times 10^{-8}\ MPa^{-1}$ in the upper bound of the 2SD range.

Table 4 Wear depth range based on [13]

Unit/ µm	mean	Max(1SD)	Min(1SD)	Max(2SD)	Min(2SD)
Maximum wear depth	1.9	2.3	1.5	2.7	1.1

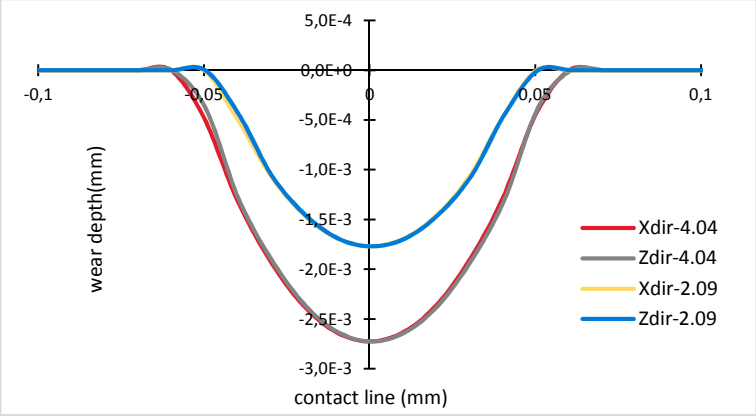

Fig. 4 Wear depth distributions of 13000 cycles along x and z direction, $\boldsymbol{k_E = 4.04 \times 10^{-8}\ MPa^{-1}, 2.09 \times 10^{-8}\ MPa^{-1}}$, respectively

It is also found that the wear damage occurs in the central of contact in Fig. 4, which is rather a characteristic of gross sliding condition than a morphology of annularity as described in [13] as in partial slip situation. Due to this disagreement, firstly the onset displacement $\delta_{sliding}$ of gross sliding in elastic condition is calculated as [12]:

$$\delta_{sliding} = \frac{3\mu P(2-\nu)}{16 a_0 G} \quad (7)$$

Where $G = \frac{E}{2(1+\upsilon)}$.

Thus, the threshold of displacement in the case is 0.294 μm. It means that in the elastic condition, gross sliding occurs when the applied displacement is greater than 0.294 μm. The applied displacement here is 5 μm that is 17 times larger than this threshold and gross sliding occurs. This is the case of the FE results.

Next, fretting loops are compared. In Fig. 5 (a) from [13], the fretting loop displays a typical quasi-closed line, which means only the adhesive occurs in the centre of contact surface. This micro displacement only leads to elastic deformation of the contact surface. However, the fretting loops of Fig. 5 (b) based on the FEM results after both 1000 and 13000 cycles, show quasi-rectangular shapes revealing that the entire bulks is sliding with each other, i.e. gross sliding condition. Meanwhile, with increasing number of cycles, the dissipated energy increases. This tendency was also found in aluminium alloy [19].

The possible reasons causing the difference between experiment and FE model in fretting loops maybe explained from two points as follows: a) the material property used is elastic with both wear coefficient while plastic deformation occurs according to the material property. Therefore fretting wear in plastic deformation is studied in the next section. b) in this paper, Coulomb law is used for contact problem. However, some researchers [20] found that this friction law is not suitable for describing the transition from 'static' to 'dynamic' friction. Ciavarella [20] proposed an 'adhesive model' that the Griffith condition is employed in the inception of slip and the Coulomb law is used in slip condition. The stick region is about 10-20% larger than the prediction based on Coulomb law. In the experiment, it was adhesive condition while the FE result showed slip condition. Based on the study of Ciavarella, using Griffith model may improve FE model. Further study should be done in the future.

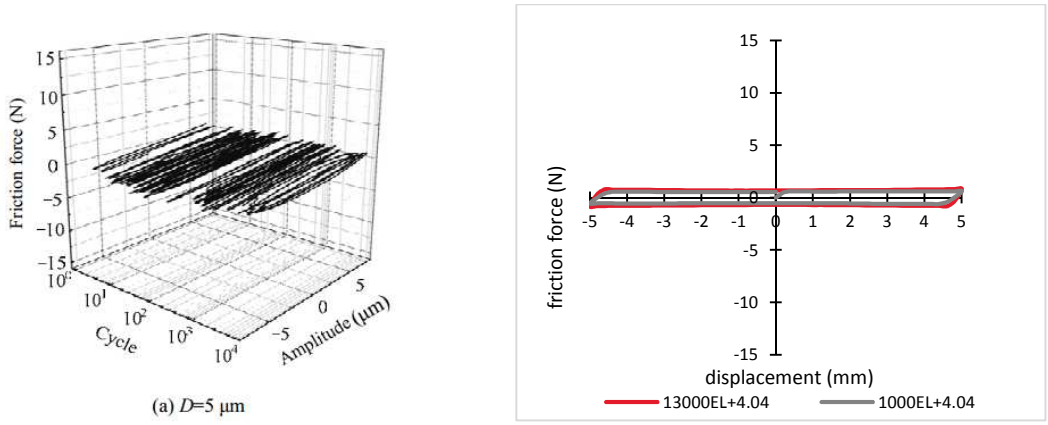

(a) (b)

Fig. 5 Fretting loops: (a) experimental results [13], (b) fretting loops after 1000 cycles and 13000 cycles in elastic condition based on FEA, $k_E = 4.04 \times 10^{-8}\ MPa^{-1}$

3.3 Comparison between elastic model and elastic-perfectly-plastic model

The comparison of fretting loops after 1000 cycles in plastic model and elastic model is plotted in **Fig. 6**. All these loops presented the quasi-rectangular shape. In both k_E cases, the friction force of plastic condition is increasing comparing to elastic condition, with little changes in the displacement. Thus the dissipated energy, the area of the fretting loop, in plastic condition is $16.54 \times 10^{-6} J$ and the elastic case is $11.07 \times 10^{-6} J$. Meanwhile, the friction force and the dissipated energy are independent of the wear coefficient.

Since part of dissipated energy is consumed for wear, the wear depths of FE model with different material behaviours are compared in **Fig. 7**. In the plastic deformation condition, the wear depth is obtained by subtraction of plastic deformation (shown in Fig. 3) from the displacement of bottom surface along y direction after unloading. It is found that:

1) In the same material behaviour condition, the wear depth increases with rising wear coefficient, while the wear width has little changes.
2) When the material behaviour changes from elastic to plastic and keeps the same wear coefficient, the wear width increases.

3) The wear depth in elastic case is more sensitive to the wear coefficient: wear depth of central point is growing by 66.5% while it is only 15.1% in plastic case, in which situation that the wear coefficient rises from $2.09 \times 10^{-8}\ MPa^{-1}$ to $4.04 \times 10^{-8}\ MPa^{-1}$. Meanwhile, in the lower wear coefficient case, the maximum wear depth of plastic case is larger than the elastic one. However, when the wear coefficient increases, the wear of elastic case gets more serious than the plastic one, especially at the centre of contact.
4) The profiles of wear scars are different in these two material behaviour conditions. The maximum wear depth in elastic model is in the centre of contact surface and decreased gradually to the contact edge, as 'U' shape. In plastic condition, however, the maximum depth is distributed at the contact edge and flattens in the centre of the contact surface, as 'W'. This wear profile is similar as the wear scar shape of partial slip condition. In this condition, maximum wear damage is in the edge of contact and little damage happens at the contact centre. The ploughing effect presents in the edge of wear scar due to the plastic deformation, which was also reported in [21, 22].

In the end, the wear scar including plastic deformation is displayed in **Fig. 8**. The shapes of wear scars in both material cases are same as 'U', but plastic deformation brings more scar depth and width. Again, the wear coefficient in elastic condition plays more important role on the wear depth than in the plastic case. It should be mentioned that the wear scar displayed in the plastic case is much larger than the elastic case which without plastic deformation. In this condition, the wear coefficient calculated by plastic deformed wear volume would be much higher than the real case.

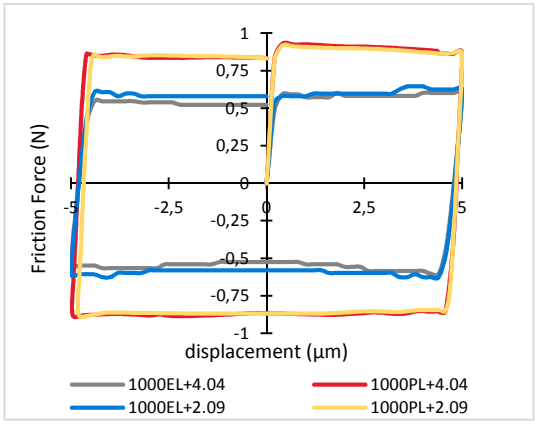

Fig. 6 Fretting loops of 1000 cycles in elastic and elastic perfectly plastic conditions

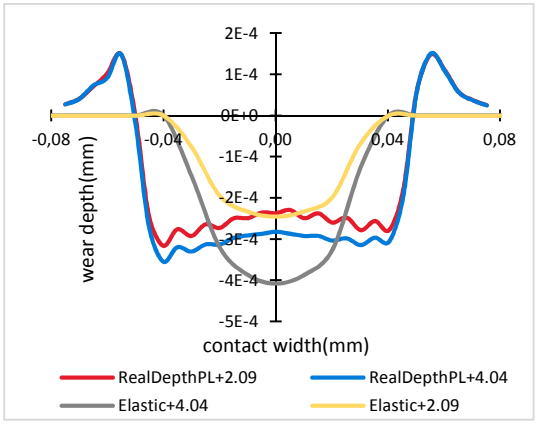

Fig. 7 Wear depth of 1000 cycles in elastic and elastic perfectly plastic conditions, along x direction

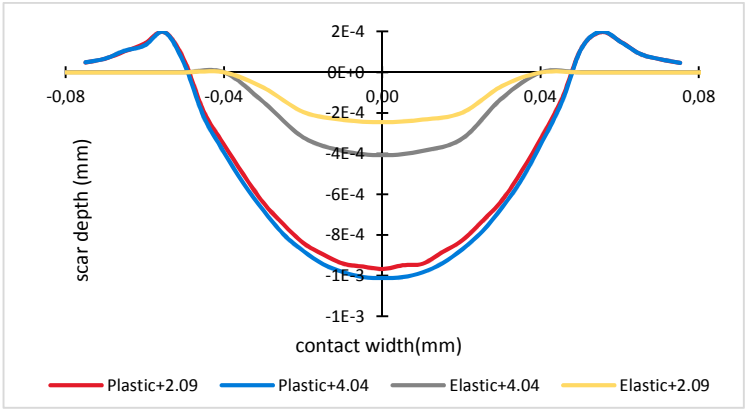

Fig. 8 wear scars after 1000 cycles in elastic and elastic perfectly plastic conditions, along x direction

4 CONCLUSION

To validate the fretting wear model and investigate the influence of material behaviour on fretting wear, the fretting wear model of wires crossed in right angle is generated in elastic behaviour with 13000 cycles and elastic perfectly plastic condition with 1000 cycles. For fretting wear model with elastic behaviour, the contact pressure and contact radius are in good agreement with the Hertzian analytical solution. The wear depth of 13000 cycles simulated is in the range of experimental results. However, the shape of fretting loop is a quasi-

rectangular shape, which means that the gross sliding happens rather than the partial slip reported in the experiments, though these FEA results are in accordance with analytical solution. For the plastic model, the fretting loop also shows gross sliding characteristic, but with higher dissipated energy. Meanwhile, the maximum wear depth distribution is a circle in the plastic model instead of one point in the elastic one. In this paper, only 1000 cycles' wear scar is simulated and the future work will be the FE modelling of the whole period of fretting wear in plastic condition.

ACKNOWLEDGEMENTS

The first author would like to acknowledge the research funding from China Scholarship Council and CWO - Mobility fund of Ghent University. The third author would like to acknowledge the research funding from National Nature Science Foundation of China, China (Grant no. 51405489) and Tribology Science Fund of State Key Laboratory of Tribology (SKLTKF13A04).

5 REFERENCES

[1] Zhang DK, Ge SR, Qiang YH. Research on the fatigue and fracture behavior due to the fretting wear of steel wire in hoisting rope. Wear. 2003;255:1233-7.

[2] Cruzado A, Hartelt M, Wäsche R, Urchegui MA, Gómez X. Fretting wear of thin steel wires. Part 1: Influence of contact pressure. Wear. 2010;268:1409-16.

[3] Wang D, Zhang D, Ge S. Finite element analysis of fretting fatigue behavior of steel wires and crack initiation characteristics. Engineering Failure Analysis. 2013;28:47-62.

[4] Wang D, Zhang D, Zhang Z, Ge S. Effect of various kinematic parameters of mine hoist on fretting parameters of hoisting rope and a new fretting fatigue test apparatus of steel wires. Engineering Failure Analysis. 2012;22:92-112.

[5] Wang D, Zhang D, Ge S. Effect of displacement amplitude on fretting fatigue behavior of hoisting rope wires in low cycle fatigue. Tribology International. 2012;52:178-89.

[6] Wang D, Zhang D, Zhao W, Ge S. Quantitative analyses of fretting fatigue damages of mine rope wires in different corrosive media. Materials Science and Engineering: A. 2014;596:80-8.

[7] Cruzado A, Urchegui MA, Gómez X. Finite element modeling and experimental validation of fretting wear scars in thin steel wires. Wear. 2012;289:26-38.

[8] Cruzado A, Leen SB, Urchegui MA, Gómez X. Finite element simulation of fretting wear and fatigue in thin steel wires. International Journal of Fatigue. 2013;55:7-21.

[9] Cruzado A, Urchegui MA, Gómez X. Finite element modeling of fretting wear scars in the thin steel wires: Application in crossed cylinder arrangements. Wear. 2014;318:98-105.

[10] Wang D, Zhang D, Wang S, Ge S. Finite element analysis of hoisting rope and fretting wear evolution and fatigue life estimation of steel wires. Engineering Failure Analysis. 2013;27:173-93.

[11] Vingsbo O, Söderberg S. On fretting maps. Wear. 1988;126:131-47.

[12] Giannakopoulos AE, Suresh S. A three-dimensional analysis of fretting fatigue. Acta Materialia. 1998;46:177-92.

[13] Shen Y, Zhang D, Ge S. Effect of fretting amplitudes on fretting wear behavior of steel wires in coal mines. Mining Science and Technology (China). 2010;20:803-8.

[14] Wang D, Magd Abdel Wahab, LL Wang, XW Li, ZC Zhu, DK Zhang, and XB Mao. Finite element analysis of fretting fatigue of fretted wires. In: Wahab MA, editor. 4th International Conference on Fracture Fatigue and Wear. Ghent2015. p. 135-42.

[15] Yue T, Abdel Wahab M. Finite element analysis of stress singularity in partial slip and gross sliding regimes in fretting wear. Wear. 2014;321:53-63.

[16] Argatov II, Gómez X, Tato W, Urchegui MA. Wear evolution in a stranded rope under cyclic bending: Implications to fatigue life estimation. Wear. 2011;271:2857-67.

[17] Popov VL. CONTACT MECHANICS AND FRICTION: Springer-Verlag Berlin Heidelberg; 2010.

[18] Cumming G, Fidler F, Vaux DL. Error bars in experimental biology. The Journal of Cell Biology. 2007;177:7-11.

[19] Zhou Z, Fayeulle S, Vincent L. Cracking behaviour of various aluminium alloys during fretting wear. Wear. 1992;155:317-30.

[20] Ciavarella M. Transition from stick to slip in Hertzian contact with “Griffith” friction: The Cattaneo–Mindlin problem revisited. Journal of the Mechanics and Physics of Solids. 2015;84:313-24.

[21] Mohd Tobi AL, Ding J, Bandak G, Leen SB, Shipway PH. A study on the interaction between fretting wear and cyclic plasticity for Ti–6Al–4V. Wear. 2009;267:270-82.

[22] Li J, Lu YH. Effects of displacement amplitude on fretting wear behaviors and mechanism of Inconel 600 alloy. Wear. 2013;304:223-30.